Dynamics of Pipes Conveying Two-Phase Flows

Final Project

ME 506: Two-Phase Flow and Heat Transfer
Department of Mechanical Engineering, Purdue University

Nirajan Adhikari
nadhika@purdue.edu

Julien Brillon
jbrillon@purdue.edu

Troy Tonner
tonner@purdue.edu

December 9, 2019

Contents

1 Introduction

1.1 Brief Background and Significance of the Problem

The dynamics of pipes conveying single-phase flows is a problem that has been studied in depth and is fairly understood. However, the dynamic response of the pipe conveying two-phase flows does not translate well from one-phase flows.

The dynamic stability of a pipe considers the effects of forces, such as those caused by internal flow, acting on a pipe. A force can cause vibrations in a pipe with different frequencies being excited by different flow characteristics. The excited frequencies can lead to the vibrations growing causing different types of instabilities. The instabilities usually fall into the following two categories: buckling which is a divergence instability and fluttering which is an oscillatory instability.

The poor translation from one-phase flow to two-phase flow makes physical sense. Two-phase flows have different flow regimes, heterogeneous physical properties, and non-uniform velocities. The heterogeneity of a two-phase system can impart harmonic-like stresses on a pipe when considering flows like adiabatic bubbly flow. The stresses can lead to excitation of different modes and frequencies at lower velocities which can lead to instabilities more easily. Various experimental and theoretical studies have shown the presence of these studies in a pipe conveying one or two-phase flows and are listed in Table (1.2).

The idea of flow induced instabilities on a pipe was originally studied for three main reasons: intrigue, interesting mathematical application, and unique boundary conditions that could be applied [25]. Over time, the problem developed from theoretical pursuit to application when considering observable behaviors, such as the snake-like oscillation of a garden-hose or fire-hose, and vibrations in above-ground pipelines [3]. Applications continue to grow (e.g. heat ex-changers) especially when entering into the two-phase flow regime of the problem. The significance is clear to see when the whole body of work of the problem is considered.

A brief overview for the procedure is that two problem set-ups were considered in the current work, a flexible pipe/tube that is either: (1) fixed at the top and free at the bottom (cantilever) or (2) fixed at both ends (clamped). In both cases the two-phase flow is flowing downward. The dynamic response of fluid-structure interaction is carried out by deriving the equation of motion (EOM) and performing the frequency analysis of the system. The EOM represents the interaction of the fluid system with the structural system and the dynamic response can be easily determined using analytical methods or numerical methods. In this study, we use the most popular numerical method; that is the Galerkin method to study the dynamic response of a pipe conveying two-phase flows. The Galerkin method applied to the nondimensional form of the EOM leads to a system of ODEs which can be solved as an eigen-value problem from which the complex frequency representing different modes of vibration can be determined. The dynamic stability of the system can be analyzed via Argand diagrams of the complex frequency for an increasing variable such as flow velocity to demonstrate the behavior of the system as that parameter is increased. The following sections will elaborate on this stability analysis, our modelling approach, instabilities, and the two-phase results.

1.2 Literature Review

Year	Authors	Problem	Remarks	Ref.
1939	Bourrières	Beam-like Structure Conveying Fluid	Examined the Flutter Instability both Experimentally and Theoretically; Derived the Linearized EOM	[5]
1951	Feodos'ev	Derived EOM for a Pipe with Simply-Supported Ends	Showed for High Velocities that the Pipe may Buckle	[10]
1955	Long	Cantilevered Pipes Conveying Fluids	Small Velocities so Oscillations were not Present; Different Boundary Conditions then Bouurières	[21]
1966	Gregory and Paidoussis	Experimentally and Theoretically Studied Sufficiently High Velocities in Cantilever Pipes	Showed that Cantilever Pipes were Subject to both Buckling and Flutter Instabilities	[12],[11]
1968	Naguleswaran and Williams	Theoretically and Experimentally Investigated Lateral Vibration of a Pipe for Pinned-Pinned, Fixed-Fixed, and Pinned-Fixed	Studied the Effect of Internal Pressure, Pipes with both Ends Supported may Buckled due to Internal Pressure Despite Low Flow Velocities	[23]
1969	Thurman and Mote	Non-linear Analysis for Simply-Supported Pipe	Non-linear Terms Importance Increases with Increasing Flow Velocity	[29]
1971	Chen	Simply-Supported Pipes with a Time-Dependent Harmonic Velocity	Determined Boundaries of Stability-Instability Regions, Combination Resonances are Possible	[7]
1974	Paidoussis and Issid	Theoretically Extends and Correct Chen's Work; Constant and Harmonic Flow Velocity: Pinned-Pinned Pipes and Cantilevered Pipes	Fixed End Pipes are Capable of Mode Coupling Flutter, but Cantilevered is only Exposed to Flutter of the First Degree of Freedom; Dissipative Forces Dampen Parametric Instability; Effectiveness of Dissipative Forces Decreases with Increasing Flow Velocity	[25]

Table 1.1: Tabulated Literature Review of One-Phase Flow Systems

Year	Authors	Problem	Remarks	Ref.
1973	Hara	Theoretically Studied Two-Phase Flow Induced Vibrations	Neglects Gravity, Friction on Inside Wall, and Axial Force at Both Ends of Pipe; Flow Induced Vibrations are Dominantly caused by the periodic two-phase mass flow	[15]
1975	Hara	Theoretical and Experimental Parallel Two-Phase Flow Induced Vibrations of a Fuel Pin	Similar Conclusions to Previous Work, but for a Different System	[17],[16]
1979	Hara	Theoretical Analysis of Two-Phase Flow on Fuel Pin Structural Dynamics	Considers Slug Flow Regime; Galerkin Method	[18]
1989	Chen	Reviews Two-Phase Flow-Induced Vibrations	Discusses: Added Mass and Damping, Cross-flow, and Axial-Flow	[8]
2002	Gulyayev and Tolbatov	Numerical Modeling of Non-Homogeneous Boiling Flows	Straight and Curved Pipes; Velocity of Flow; Size of Fluid Clots and Vapor Cavities	[13]
2003	Pettigrew and Taylor	Flow-Induced Vibrations in Shell and Tube Heat Exchangers	Developed Guidelines to Prevent Tube Failures	[27],[28]
2004	Gulyayev and Talbatov	Numerical Modeling of Non-Homogeneous Boiling Flows	Spiral Tubing	[14]
2004	Monette and Pettigrew	Experimental and Analytical Two-Phase Flow-Induced Dynamic Stability for a Vertical Cantilever Pipe	Range of Flow Velocities; Range of Void Fractions; Varied Pipe Diameters, Lengths, Flexural Rigidities	[22]
2009	Béguin, Anscutter, Ross, Pettigrew, and Mureithi	Two-Phase Vertical Internal Flow	Relates Damping in the Bubbly Flow Regime to Interface Surface Area	[6]
2015	An and Su	Analytically and Numerically Investigated the Dynamic Behavior of Pipes Conveying Two-Phase Flows	Applied Generalized Integral and Transform Technique; Vertical Pipe with Clamped-Clamped Boundary Conditions	[2]
2017	Adegoke and Oyediran	Analyzed Nonlinear Vibrations of Cantilever Pipes Conveying Pressurized Steady Two-Phase with Thermal Loading	Applied Hamilton's Mechanics;Mutilple-Scale Pertubartion Technique	[1]
2018	Liu and Wang	Horizontal Cantilevered Pipe; Slug Flow	Natural Frequency Analysis	[20]
2018	Bai, Xie, Gao, and Xu	Vertical Cantilever Pipe	Consider Density Variation; Derived from New Model from Bernoulli-Euler Beam Model and Newton's Second Law	[4]
2019	Ebrahimi-Mamaghani et al.	Vertical Cantilever Pipes	Consider Upward and Downward Flow; Applied Galerkin Method	[9]
2020	Li, An, Duan, and Su	Clamped-Clamped Vertical Pipe	Applied Damping Model; Used GITT method and Parametric Studies; Ocean Application Focused	[19]

Table 1.2: Tabulated Literature Review of Two-Phase Flow Systems

2 Equation of Motion

A fluid-structure interaction system is modeled by formulating an Equation of Motion (EOM) for a small deformation of the structural element due to the forces imparted by the fluid element. A typical free body diagram for a small deflection of a pipe system conveying 1ϕ fluid is shown in Fig. (2.1).

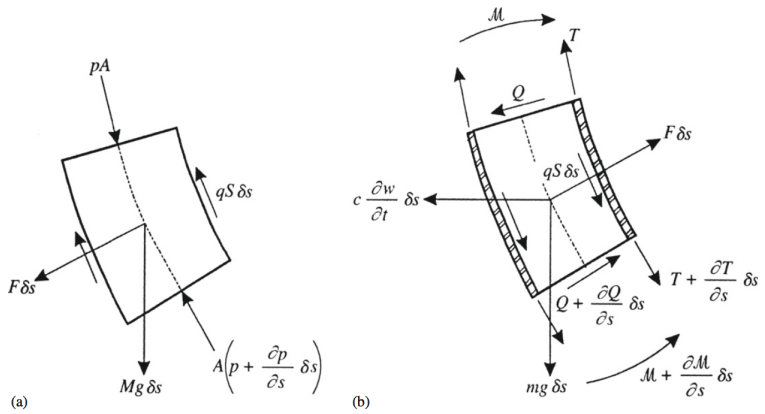

Figure 2.1: FBD of Fluid/Pipe Element [26]

Under the assumption that the liquid and gas phases impart forces independently on the pipe system, the EOM for a small transverse deflection of a pipe conveying 2ϕ flow can be represented as [22]:

$$\underbrace{EI(1+\mu i)\frac{\partial^4 y}{\partial x^4}}_{\textbf{Elastic force}} + \underbrace{\left(m_l U_l^2 + m_g U_g^2\right)\frac{\partial^2 y}{\partial x^2}}_{\textbf{Centrifugal force}} + \underbrace{2\left(m_l U_l + m_g U_g\right)\frac{\partial^2 y}{\partial x \partial t}}_{\textbf{Coriolis force}}$$
$$+ \underbrace{\left(m_p + m_l + m_g\right)\frac{\partial^2 y}{\partial t^2}}_{\textbf{Inertia force}} + \underbrace{\left(m_p + m_l + m_g\right)\boldsymbol{g}\left((x-L)\frac{\partial^2 y}{\partial x^2} + \frac{\partial y}{\partial x}\right)}_{\textbf{Gravity}} = 0 \quad (1)$$

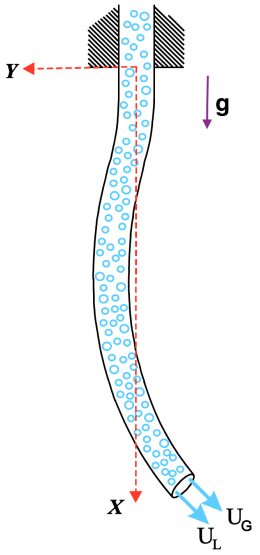

Figure 2.2: Cantilever Pipe Conveying Two Phase Flow [9]

Here, E is the materials modulus of elasticity, I is the elements second moment of area, μ is the hysteric structural damping coefficient, m_l, m_g and m_p are the mass per unit length of the liquid phase, gas phase and the pipe, respectively, U_l and U_g are the liquid phase velocity and gas phase velocity, respectively, $\mathbf{g}$ is the gravity, and L is the length of the pipe system.

Different types of forces; Elastic, Centrifugal, Coriolis, Inertia, and Gravity on a pipe conveying 2ϕ flow are identified in Eq.(1). The gravity term can be positive or negative based on the orientation of the piping system. It is positive for the vertically hanging pipe as in fig.(2.2).

To study the dynamic of the fluid-structure interaction, the EOM is usually nondimensionalize. The nondimensional parameters are as follows:

$$\xi = \frac{x}{L} \qquad \eta = \frac{y}{L} \qquad \tau = \frac{t}{T} \qquad T = L^2\sqrt{\frac{m_p + m_l + m_g}{EI}}$$
$$\beta_k = \frac{m_k}{m_p + m_l + m_g} \qquad u_k = U_k L\sqrt{\frac{m_k}{EI}} \qquad \gamma = \boldsymbol{g}L^3\sqrt{\frac{m_p + m_l + m_g}{EI}} \quad (2)$$

where $k = l, g$ (denoting the phases). Using the above listed nondimensional parameters, the EOM in eq.(1) can be nondimensionalize to get eq.(3).

$$(1+\mu i)\,\eta'''' + \left(u_l^2 + u_g^2\right)\eta'' + 2\left(\sqrt{\beta_l}u_l + \sqrt{\beta_g}u_g\right)\dot{\eta}' + \ddot{\eta} + \gamma\left[(\xi - 1)\eta'' + \eta'\right] = 0 \quad (3)$$

2.1 Two Phase (2ϕ) Flow Parameters

The relation between the liquid and gas phases are often defined based on the following 2ϕ flow parameters:

- Volumetric quality: $\epsilon = \frac{Q_g}{Q}$
- Void fraction: $\alpha = \frac{A_g}{A}$
- Slip ratio: $K_s = \frac{U_g}{U_l}$

where, Q is the volumetric flow rate, A_g is the cross-sectional area occupied by the gas phase, and A is the total cross-sectional area of the pipe. These parameters are related by the following:

$$\frac{1-\epsilon}{\epsilon} = \left(\frac{1-\alpha}{\alpha}\right)\frac{1}{K_s} \tag{4}$$

Since the velocity is different for different phases, slip ratio parameter is often introduced to relate the velocity of liquid and gas phases. The slip ratio in a vertical hanging pipes for air-water flow is given by [22]:

$$K_s = \sqrt{\frac{\epsilon}{1-\epsilon}} \tag{5}$$

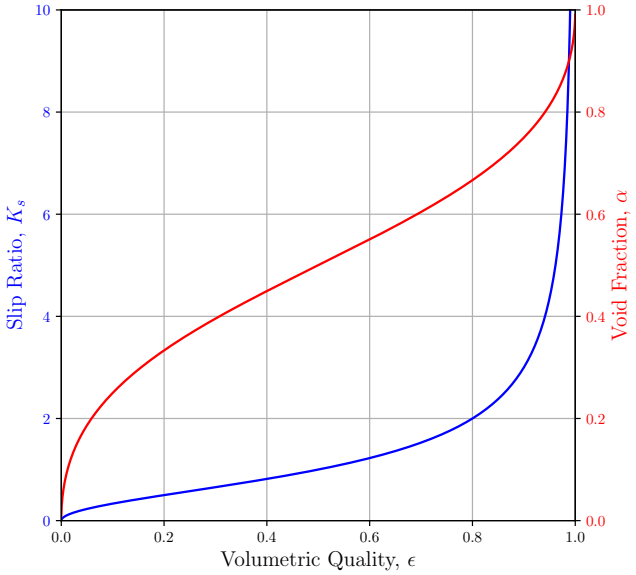

Figure 2.3: Variation of 2ϕ Flow Parameters

In a vertically hanging pipe, due to the buoyancy effects, the gas phase velocity will be lower than the liquid phase for small void fraction, evident in fig.(2.3). The gas phase velocity will eventually be greater than liquid velocity at higher void fraction.

2.2 Relation between 1ϕ and 2ϕ Flow

The mass ratio parameter β changes with the increase in void fraction α. Thus, a proper relation for the mass ratio between 1ϕ and 2ϕ system needs to be established if one consider comparing the 1ϕ system with 2ϕ. Between these two systems, the mass per unit length of the pipe remains a constant and the variation of mass ratio of the liquid phase (β_l) with change in void fraction can be derived as follows:

For 1ϕ (liquid only):

$$\beta_{l_0} = \frac{m_l}{m_p + m_l} \tag{6}$$

Thus, we can write:

$$\frac{m_p}{A} = \rho_l\left(\frac{1-\beta_{l_0}}{\beta_{l_0}}\right) \tag{7}$$

where, ρ is the density. For 2ϕ:

$$\beta_l = \frac{m_l}{m_p + m_l + m_g} \tag{8}$$

$$\beta_l = \frac{\rho_l(1-\alpha)}{\frac{m_p}{A} + \rho_l(1-\alpha) + \rho_g\alpha} \tag{9}$$

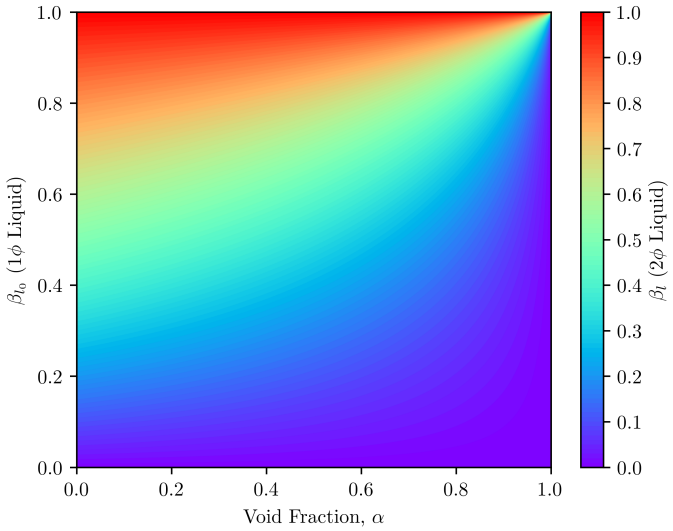

Figure 2.4: Variation of β_l vs β_{l_0} and α

Fig.(2.4) shows the variation of liquid mass ratio with void fraction for a given liquid mass ratio in 1ϕ. Extreme care needs to be exercised while using this relation between phases. The formulation of the equations derived here assumes that there is no variation in the properties across the length of a pipe. In reality, we know that different flow regimes- bubbly, slug, churn, annular- are usually encountered with the increase in void fraction. The flow is usually not uniform throughout the length in churn and slug flow regime, evident in

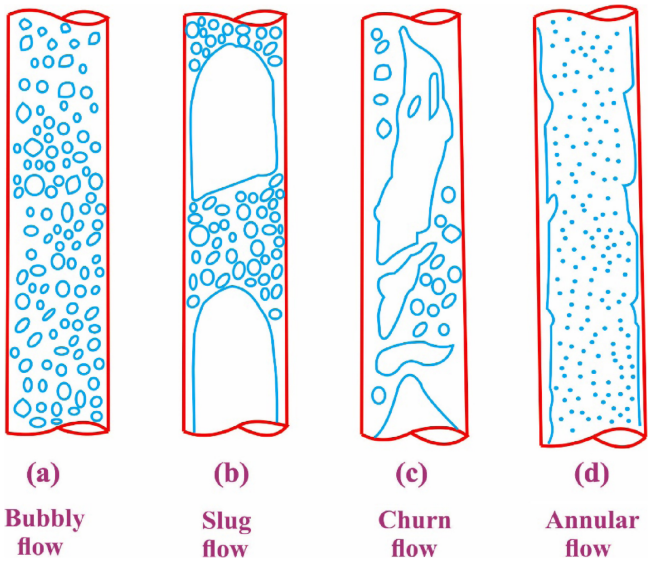

Figure 2.5: Various Flow Regimes in 2ϕ Flow [9]

fig.(2.5). Thus, the relation between 1ϕ and 2ϕ system should be used with extreme caution. Using eq.(2) and eq.(4) it can be shown that:

$$\beta_g = \left(\frac{\rho_g \epsilon_g}{\rho_l (1-\epsilon_g) K_s}\right) \beta_l \qquad u_g = u_l \sqrt{K_s \left(\frac{\rho_g \epsilon_g}{\rho_l (1-\epsilon_g)}\right)} \tag{10}$$

Using eq.(10) in eq.(3), the final form of nondimensional EOM becomes:

$$(1+\mu i)\,\eta'''' + u_l^2 \left[1 + K_s \left(\frac{\rho_g \epsilon_g}{\rho_l (1-\epsilon_g)}\right)\right] \eta'' + 2\sqrt{\beta_l} u_l \left[1 + \frac{\rho_g \epsilon_g}{\rho_l (1-\epsilon_g)}\right] \dot{\eta}' + \ddot{\eta} + \gamma \left[(\xi - 1)\eta'' + \eta'\right] = 0 \tag{11}$$

3 Numerical Approach

The nondimensional EOM given by eq.(11), was solved numerically using Galerkin method. To apply this method, we consider a general solution of the form:

$$\eta(\xi, \tau) = \sum_{r=1}^{n} \phi_r(\xi) q_r(\tau) \tag{12}$$

where, $\phi_r(\xi)$ are the orthogonal eigen-functions of the system, given as:

$$\phi_r(\xi) = \cosh(\lambda_r \xi) - \cos(\lambda_r \xi) - \sigma_r \left\{\sinh(\lambda_r \xi) - \sin(\lambda_r \xi)\right\} \tag{13}$$

$$\sigma_r = \begin{cases} \dfrac{\sinh(\lambda_r) - \sin(\lambda_r)}{\cosh(\lambda_r) - \cos(\lambda_r)} & \text{for clamped pipes (fixed-fixed)} \\ \dfrac{\sinh(\lambda_r) - \sin(\lambda_r)}{\cosh(\lambda_r) + \cos(\lambda_r)} & \text{for cantilever pipes (fixed-free)} \end{cases} \tag{14}$$

where λ_r are the eigenvalues of r-th mode of the system, obtained from the system's frequency equation:

$$\left.\begin{array}{l} \cos(\lambda_r)\cosh(\lambda_r) - 1 \\ \cos(\lambda_r)\cosh(\lambda_r) + 1 \end{array}\right\} = 0 \quad \begin{array}{l} \text{for clamped pipes (fixed-fixed)} \\ \text{for cantilever pipes (fixed-free)} \end{array} \tag{15}$$

numerically via *Newton-Raphson*'s root-finding method. **Note:** For accurate results, a 10 mode approximation was used i.e. $n = 10$ as it yields results accurate to three significant digits [24]. The weak formulation of the nondimensional EOM was obtained by substituting eq.(12), multiplying by a trial function (chosen to be same as the eigenfunctions), and integrating over the standard domain $\xi \in [0, 1]$. Thus, using Galerkin method, the PDE (EOM) is transformed into a system of ODEs as:

$$[M]\,\ddot{\boldsymbol{q}}(\tau) + [C]\,\dot{\boldsymbol{q}}(\tau) + [K]\,\boldsymbol{q}(\tau) = \boldsymbol{0} \tag{16}$$

where $[M]$ is the mass matrix, $[C]$ is the damping matrix, $[K]$ is the stiffness matrix and $\boldsymbol{q}$ is:

$$\boldsymbol{q}(\tau) = \begin{bmatrix} q_1(\tau) \\ q_2(\tau) \\ \vdots \\ q_n(\tau) \end{bmatrix} \tag{17}$$

Note: the eigenfunctions are orthogonal, thus:

$$\int_0^1 \phi_s \phi_r d\xi = \delta_{sr} \tag{18}$$

where δ_{sr} is the Kronecker delta. Additionally, we can see that:

$$\phi_r(\xi)'''' = \lambda_r^4 \phi_r(\xi) \tag{19}$$

Using the above two relations, the respective matrix elements in eq.(16) are as follows:

$$M_{sr} = \delta_{sr} \tag{20}$$

$$C_{sr} = 2\sqrt{\beta_l} u_l \left[1 + \frac{\rho_g \epsilon_g}{\rho_l (1-\epsilon_g)}\right] b_{sr} \tag{21}$$

$$K_{sr} = (1+\mu i)\,\lambda_r^4 \delta_{sr} + u_l^2 \left[1 + K_s \left(\frac{\rho_g \epsilon_g}{\rho_l (1-\epsilon_g)}\right)\right] c_{sr} + \gamma\,(d_{sr} - c_{sr} + b_{sr}) \tag{22}$$

where

$$b_{sr} = \int_0^1 \phi_s \phi_r' d\xi \tag{23}$$

$$c_{sr} = \int_0^1 \phi_s \phi_r'' d\xi \tag{24}$$

$$d_{sr} = \int_0^1 \phi_s \xi \phi_r'' d\xi \tag{25}$$

Note: the integration was performed numerically via the *composite trapezoidal rule*.

The second-order system of ODEs given by eq.(16) can be transformed into a first-order system of ODEs in the following manner:

$$[B]\,\dot{\boldsymbol{Z}}(\tau) + [E]\,\boldsymbol{Z}(\tau) = \boldsymbol{0} \tag{26}$$

where:

$$[B] = \begin{bmatrix} 0 & [M] \\ [M] & [C] \end{bmatrix} \qquad [E] = \begin{bmatrix} -[M] & 0 \\ 0 & [K] \end{bmatrix} \qquad \boldsymbol{Z}(\tau) = \begin{bmatrix} \boldsymbol{q}(\tau) \\ \dot{\boldsymbol{q}}(\tau) \end{bmatrix} \tag{27}$$

Assuming the solution form to be $\boldsymbol{Z}(\tau) = \boldsymbol{a} e^{i\omega\tau}$, substituting into eq.(26), we arrive to the standard eigenvalue problem:

$$([Y] - i\omega\,[I])\,\boldsymbol{a} = \boldsymbol{0} \tag{28}$$

where $[Y] = -[B]^{-1}[E]$. The complex frequency ω and respective eigenvectors $\boldsymbol{a}$ can be determined by solving the eigenvalue problem eq.(28) for a fixed u_l.

4 Results

A cantilever pipe system and a clamped pipe system were considered in this work and the dynamic response was investigated to investigate instability modes, critical flow velocity, and the effects of 2ϕ flow parameters. The 2ϕ flow is composed of a water-air mixture. All the test cases in this study were investigated using a 10 mode Galerkin approximation. The developed Galerkin solver was verified by comparing the 1ϕ results ($\epsilon = 0$ from the literature.

- **Case I: Vertical Hanging Cantilever Pipe (Fixed-Free)**
  - $\rho_g = 1.2$ kg/m^3, $\rho_l = 1000$ kg/m^3
  - $\mu = 0$, $\beta_{l_0} = \{0.3,\ 0.2,\ 0.65\}$, $\gamma = \{10,\ 100\}$
- **Case II: Vertically Clamped Pipe (Fixed-Fixed)**
  - $\rho_g = 1.2$ kg/m^3, $\rho_l = 1000$ kg/m^3
  - $\mu = 0$, $\beta_{l_0} = 0.645$, $\gamma = 0$

4.1 Case I: Vertical Downflow in a Cantilever Pipe

4.1.1 Verification

The frequency response of the vertical downflow cantilever pipe is presented in fig.(4.1) in the form of an Argand diagram, which is a dimensionless complex frequency plot. The positive imaginary axis represents the damping of the system's time-dependant response. The system becomes unstable when the frequency response crosses the stability line, i.e. when the imaginary component of the complex frequency, $\mathrm{Im}(\omega)$, is negative. Since, vibrations are amplified at these ($\mathrm{Im}(\omega) < 0$) frequencies.

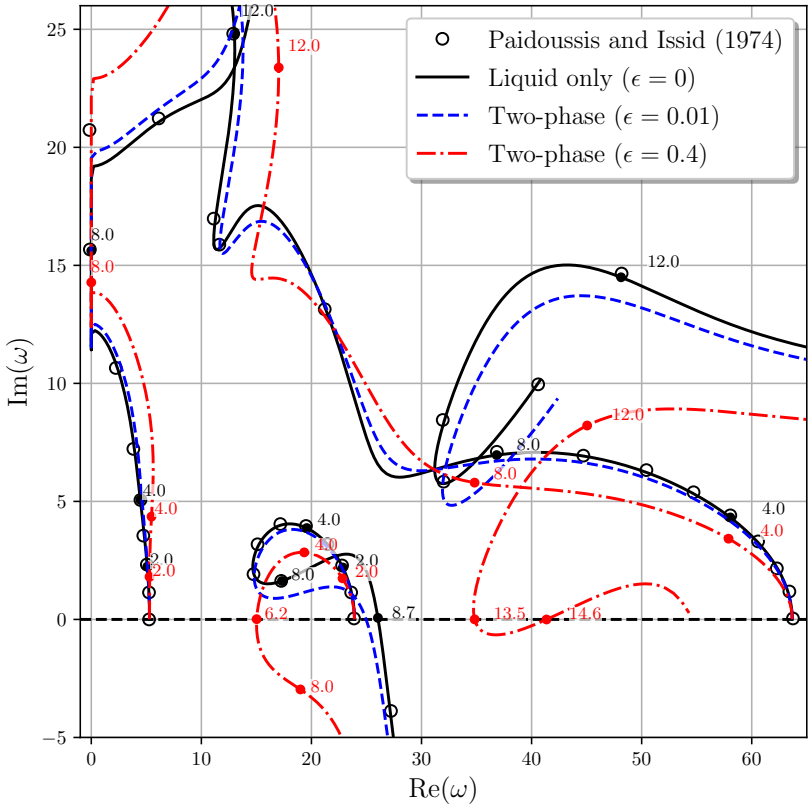

Figure 4.1: Argand diagram for Vertical Downflow Cantilever Pipe: $\beta_{l_0} = 0.3$, $\gamma = 10$, $\mu = 0$

From fig.(4.1), we see that the results for 1ϕ (liquid only) flow match well with Paidoussis and Issid (1974) [25] results. Looking at the 2ϕ flow results, we see that the frequency response starts to deviate from that of the 1ϕ flow at higher flow velocities even with slight increase in volumetric quality ($\epsilon = 0.01$) as the momentum difference between phases increases (i.e. as we increase ϵ). We note that the first and third modes are always stable (damped). However, for higher gas flow ($\epsilon = 0.4$) we see that the frequency response is considerably different than of 1ϕ flow system.

The critical velocity for the second mode instability of 2ϕ flow is $u_l^c = 6.2$ for $\epsilon = 0.4$ whereas for the 1ϕ flow we have $u_l^c = 8.7$. This type of instability is called *Hopf bifurcation* yielding single mode *flutter*. Taking a look at the fourth mode for $\epsilon = 0.4$, we see that it becomes unstable at $u_l^c = 13.5$ but restabilizes at $u_l^c = 14.6$ and ultimately becomes unstable for $u_l^c = 15.0$. This restabilization phenomena will be further discussed in later sections of the report. It should be noted for clarity that for the system to be considered unstable, at least one of it's modes must be unstable, i.e. the $\epsilon = 0.4$ system is ultimately unstable for $u_l > 6.2$.

4.1.2 1ϕ Response vs 2ϕ

The time dependant response of the nondimensional tip deflection, $\eta(1, \tau)$, given by eq.((12)), for both the 1ϕ and 2ϕ systems are shown in fig.(4.2). The nondimensional tip deflection is plotted for velocities before and after each respective system becomes unstable. From fig.(4.2)(a,b), we see the response of each system at their respective nondimensional critical liquid flow velocity, u_l^c. In addition, from fig.(4.2)(c,d) we see that to reach about the same vibration amplitude, the increase in u_l past u_l^c, Δu_l, is 0.1 for the 1ϕ system and 0.04 for the 2ϕ system. Therefore, we see that while 2ϕ effects decrease the critical flow velocity u_l^c, they also *reduce the rate of vibration amplification*. This is can be explained by the fact that the Re(ω) is smaller for two-phase systems.

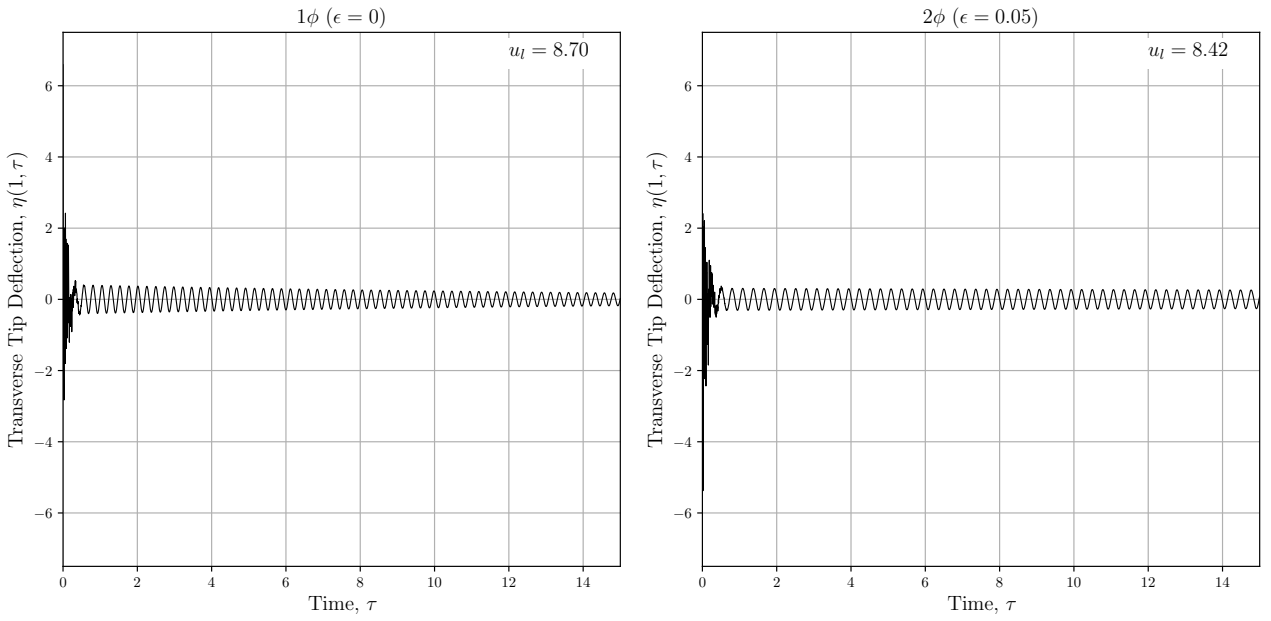

(a) 1ϕ at it's $u_l^c = 8.70$

(b) 2ϕ at it's $u_l^c = 8.42$

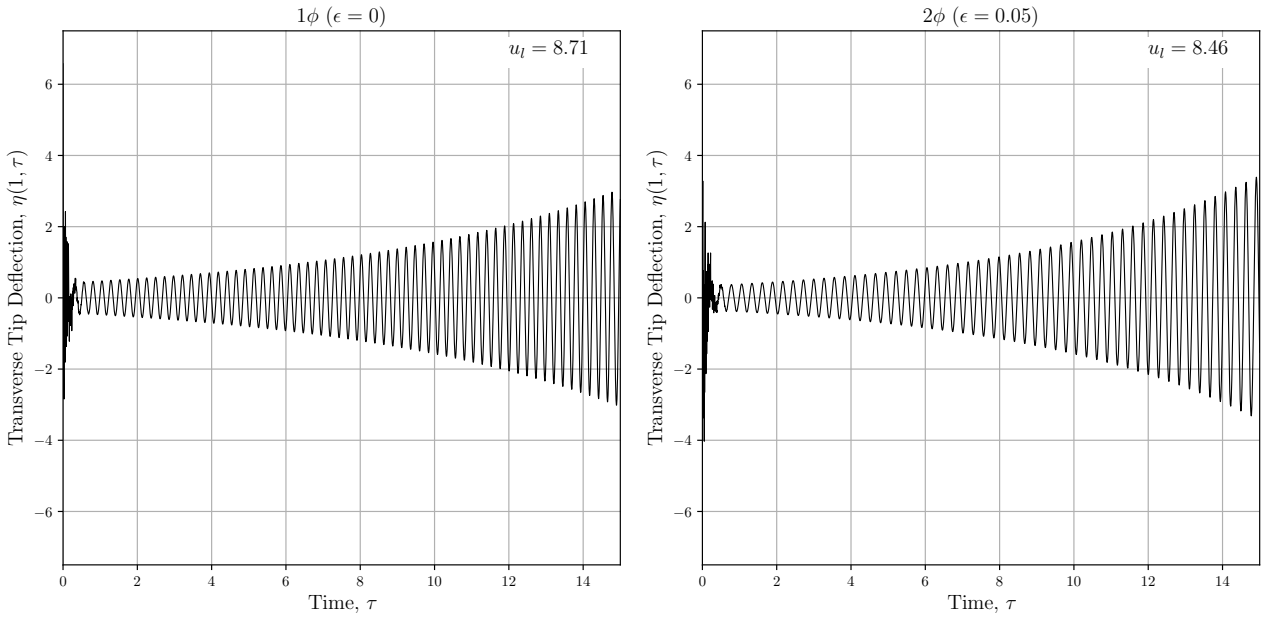

(c) 1ϕ at $u_l = 8.71$

(d) 2ϕ at $u_l = 8.46$

Figure 4.2: Comparison of 1ϕ and 2ϕ system responses

4.1.3 Importance of Volumetric Quality

The volumetric quality, ϵ, is an important parameter to study the dynamics of pipes conveying 2ϕ flows. A change in ϵ can significantly alter the dynamics of a system, as demonstrated in fig.(4.3).

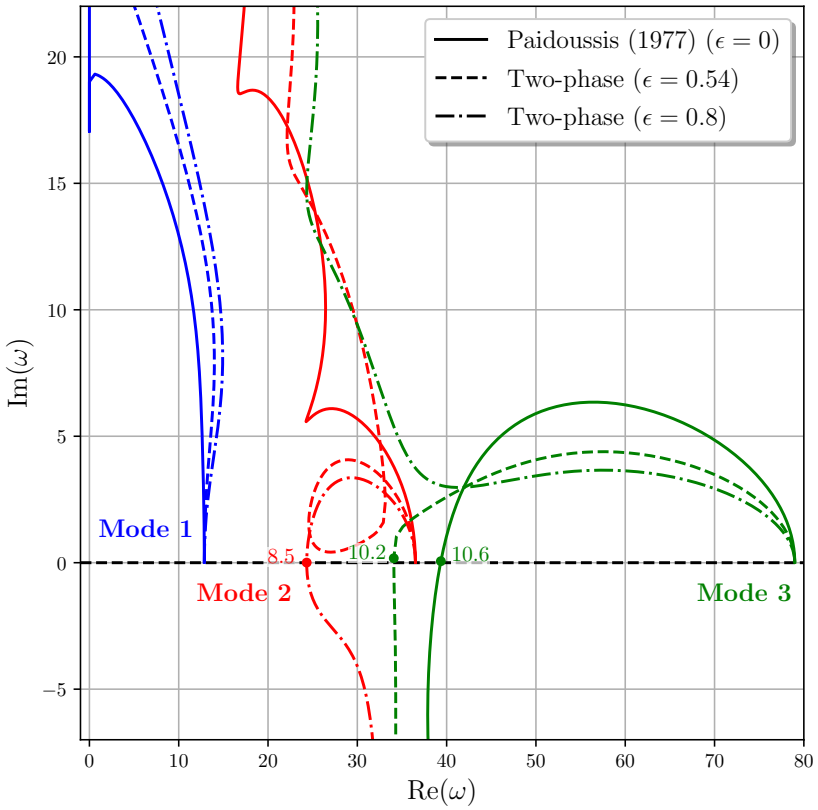

Figure 4.3: Argand diagram for Vertical Downflow Cantilever Pipe: $\beta_{l_0} = 0.2$, $\gamma = 100$, $\mu = 0$

The 1ϕ system is unstable through Mode 3 vibration but with increase in gas phase flow ($\epsilon = 0.50$), we see that the response of Mode 2 moves closer to the stability line. When gas phase flow is further increased to $\epsilon = 0.8$, the system now becomes unstable through Mode 2 vibration while Mode 3 stabilizes.

4.1.4 Restabilization Phenomena

As mentioned before, sometimes an interesting response can be encountered in a system when restabilization occurs by continuing to increasing the flow velocity after the system has become initially unstable.

A **"Z"** type frequency response indicates presence of a **unstable-stable-unstable** response; as illustrated in fig.(4.4). The fourth mode of the $\epsilon = 0.1$ system exhibits this *unstable-stable-unstable*, or "Z", response. We see that this system becomes **unstable** at $\mathbf{u_l^{c1} = 15.82}$ and **regains stability** with further increase in flow velocity at $\mathbf{u_l^{c2} = 17.0}$, and returns **unstable** at $\mathbf{u_l^{c3} = 17.39}$.

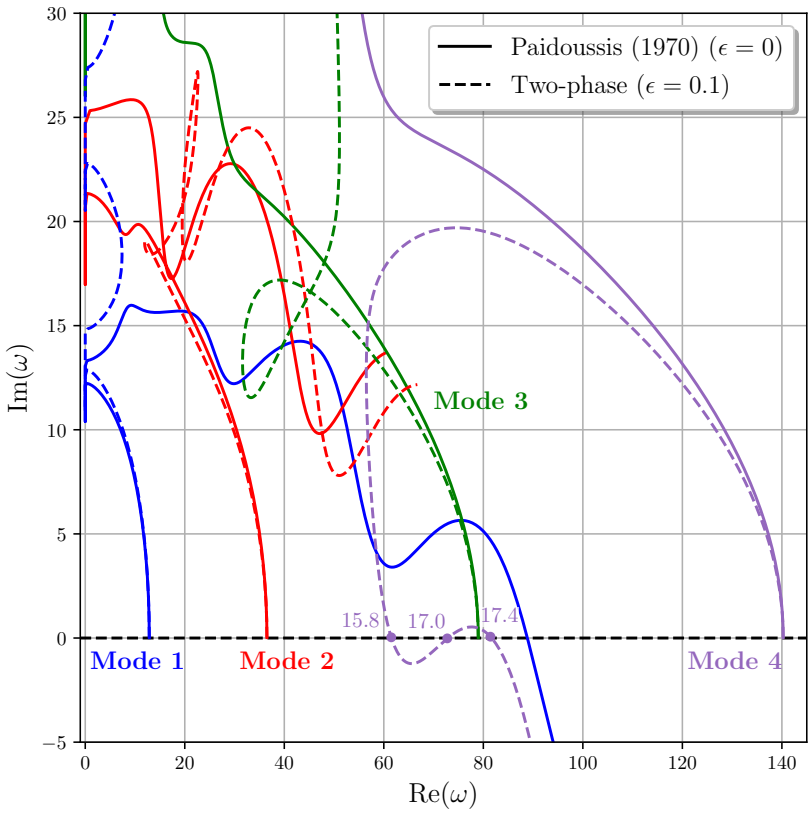

Figure 4.4: Argand Diagram for $\beta_{l_0} = 0.65$, $\gamma = 100$, $\mu = 0$

The evolution of the tip deflection with increasing flow velocity is demonstrated in fig.(4.5) and it can be seen that the tip deflection does indeed exhibit the "Z" response with varying flow velocity.

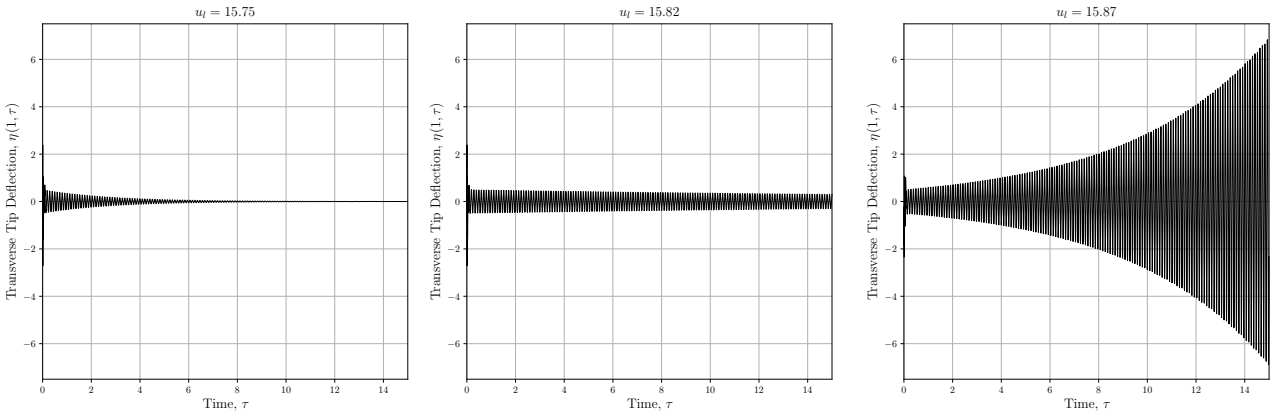

(a) $u_l = 15.75$ (b) $u_l = u_l^{c1} = 15.82$ (c) $u_l = 15.87$

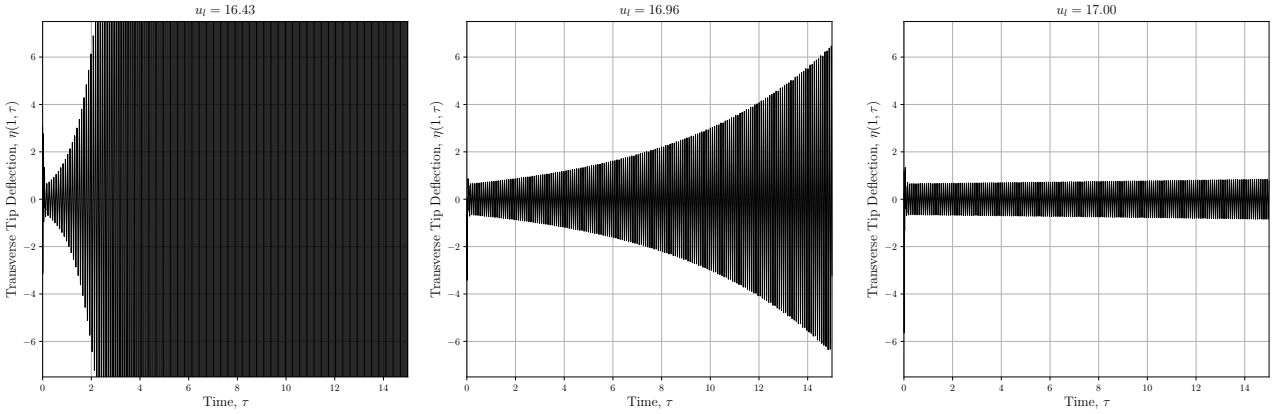

(d) $u_l = 16.43$ (e) $u_l = 16.96$ (f) $u_l = u_l^{c2} = 17.00$

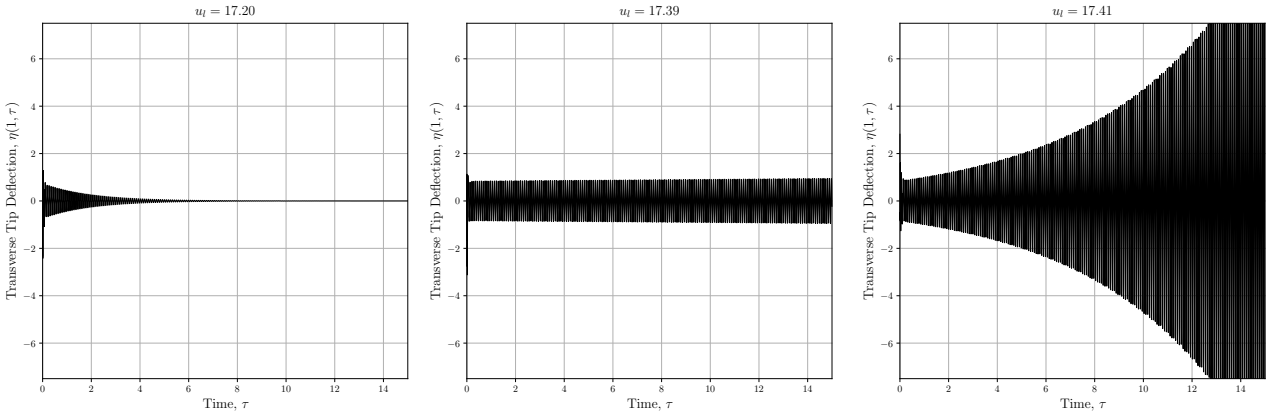

(g) $u_l = 17.20$ (h) $u_l = u_l^{c3} = 17.39$ (i) $u_l = 17.41$

Figure 4.5: Restabilizing system respone

The transient of the system's transverse deflection is shown in fig.(4.6) for u_l when the system is unstable ($u_l = 15.85 > u_l^{c1}$). This clearly illustrates the *flutter* type instability with vibration amplitude growing in time due to the absence of damping. In addition, we see that vibrations are largest at the fixed boundary ($\xi = 0$), and decrease as we move towards the tip ($\xi = 1$).

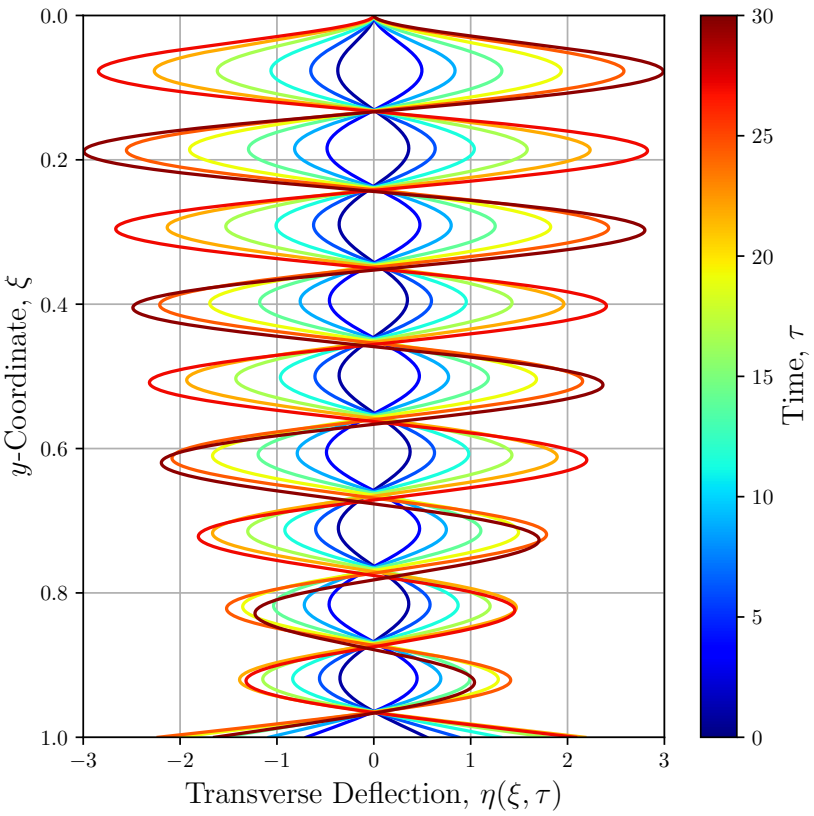

Figure 4.6: Transient of η vs ξ at $u_l = 15.85$ for $\epsilon = 0.1$, $\beta_{l_0} = 0.65$, $\gamma = 100$, $\mu = 0$

Another, feature of the "Z" type response is that the system becomes extremely sensitive to a small change in ϵ. From fig.(4.7), we see that the 3rd Mode response is almost tangent to the stability line for $\epsilon = 0.83$, whereas for $\epsilon = 0.85$ we see a drastic change in the stability of the system.

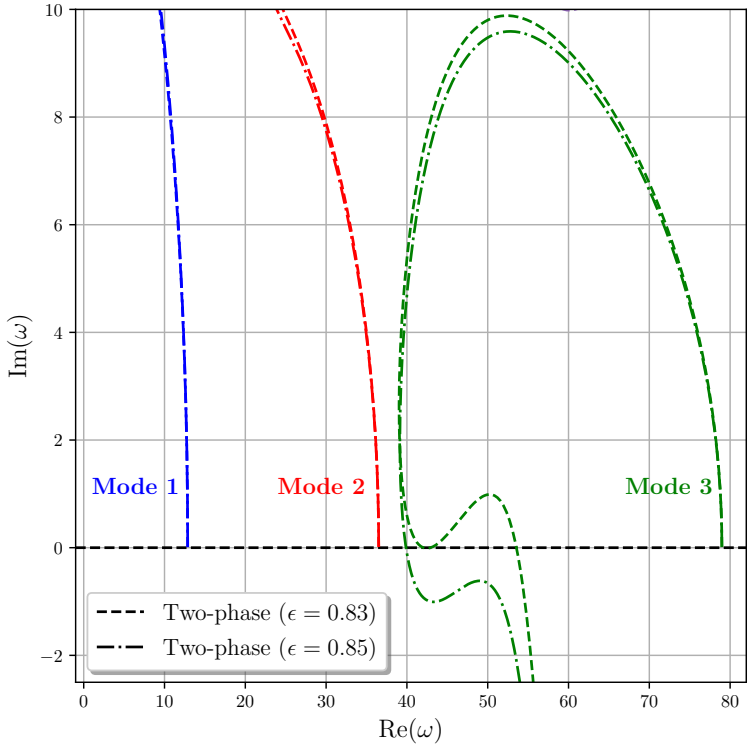

Figure 4.7: Argand Diagram for $\beta_{l_0} = 0.65$, $\gamma = 100$, $\mu = 0$

4.2 Case II: Vertical Down-Flow in a Clamped Pipe

From fig.(4.8) we observe the following: (1) the response is drastically different than that of cantilever pipes, (2) from fig.(4.8)(a) we see that for $u_l > 9.0$ modes 1 and 2 become coupled as they have the same Re(ω), (3) from fig.(4.8)(b) we see that 2ϕ reduces u_l^c of the system (with respect to the 1ϕ system).

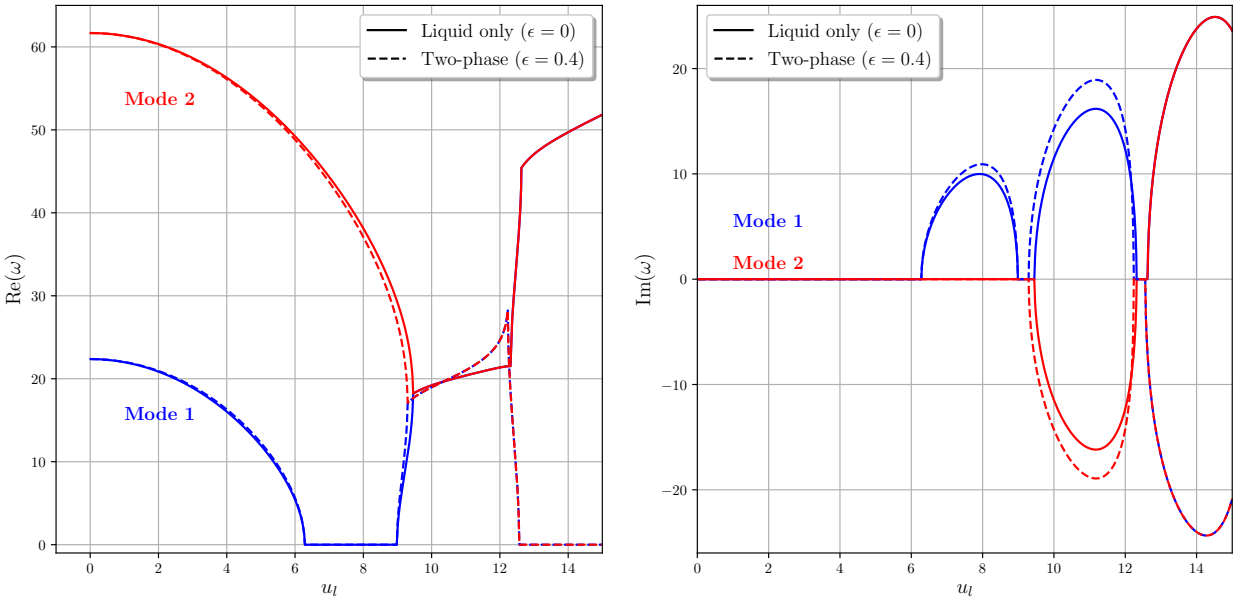

(a) Re(ω) **vs** u_l

(b) Im(ω) **vs** u_l

Figure 4.8: $\beta_{l_0} = 0.645$, $\gamma = \mu = 0$

5 Conclusion

To conclude, the dynamics of pipes conveying two-phase flows were successfully studied for both cantilever and clamped pipe systems. The complex frequency analysis of the fluid-structure interaction (FSI) was performed numerically by applying Galerkin method to the equation of motion. Through various studies, it has been shown that two-phase flow systems behave gradually different than liquid-only systems as the amount of gas phase flow (ϵ) is increased. In comparison to the liquid only system, it was found that while two-phase flow systems decrease both the critical velocity and the rate of vibration amplification of the system. The dynamic response of a pipes conveying two-phase flows is highly dependant on the degree of gas phase flow present in the system. The stability of different modes can be altered by higher degrees of gas phase present in the two-phase flow. In addition, the system critical velocity is highly sensitive to small changes in degree of gas phase present in the two-phase flow. Lastly, the dynamic response of cantilever and clamped pipes was shown to be drastically different. This project has laid the foundation for further realistic modelling of two-phase systems.

References

[1] Adegoke, A. and Oyediran, A. (2017). The analysis of nonlinear vibrations of top-tensioned cantilever pipes conveying pressurized steady two-phase flow under thermal loading. *Mathematical and Computational Applications*, 22(4):44.

[2] An, C. and Su, J. (2015). Dynamic behavior of pipes conveying gas–liquid two-phase flow. *Nuclear Engineering and Design*, 292:204 – 212.

[3] Ashley, H. and Haviland, G. (1950). Bending vibrations of a pipe line containing flowing fluid. *Journal of Applied Mechanics-Transactions of the ASME*, 17(3):229–232.

[4] Bai, Y., Xie, W., Gao, X., and Xu, W. (2018). Dynamic analysis of a cantilevered pipe conveying fluid with density variation. *Journal of Fluids and Structures*, 81:638–655.

[5] Bourrières, F.-J. and Bénard, H. (1939). *Sur un phénomène d'oscillation auto-entretenue en mécanique des fluides réels: par François-Joseph Bourrières... Préface de M. H [enri] Bénard...* E. Blondel La Rougery, Gauthier-Villars.

[6] Béguin, C., Anscutter, F., Ross, A., Pettigrew, M., and Mureithi, N. (2009). Two-phase damping and interface surface area in tubes with vertical internal flow. *Journal of Fluids and Structures*, 25(1):178 – 204.

[7] Chen, S. (1971). Dynamic stability of tube conveying fluid. *Journal of Engineering Mechanics*.

[8] Chen, S. (1989). A review of two-phase flow-induced vibration. In *Design & Analysis*, pages 107–125. Elsevier.

[9] Ebrahimi-Mamaghani, A., Sotudeh-Gharebagh, R., Zarghami, R., and Mostoufi, N. (2019). Dynamics of two-phase flow in vertical pipes. *Journal of Fluids and Structures*, 87:150–173.

[10] Feodos'Ev, V. (1951). Vibrations and stability of a pipe when liquid flows through it. *Inzhenernyi Sbornik*, 10:169–170.

[11] Gregory, R. and Paidoussis, M. (1966a). Unstable oscillation of tubular cantilevers conveying fluid. i. theory. *Proceedings of the Royal Society of London. Series A. Mathematical and Physical Sciences*, 293(1435):512–527.

[12] Gregory, R. and Paidoussis, M. (1966b). Unstable oscillation of tubular cantilevers conveying fluid ii. experiments. *Proceedings of the Royal Society of London. Series A. Mathematical and Physical Sciences*, 293(1434):528–542.

[13] Gulyayev, V. and Tolbatov, E. Y. (2002). Forced and self-excited vibrations of pipes containing mobile boiling fluid clots. *Journal of Sound and Vibration*, 257(3):425–437.

[14] Gulyayev, V. and Tolbatov, E. Y. (2004). Dynamics of spiral tubes containing internal moving masses of boiling liquid. *Journal of sound and vibration*, 274(1-2):233–248.

[15] Hara, F. (1973). A theory on the two-phase flow induced vibrations in piping systems.

[16] Hara, F. (1975a). Experimental study of the vibrations of a fuel pin model in parallel two-phase flow. In *Structural mechanics in reactor technology*.

[17] Hara, F. (1975b). A theory of the vibrations of a fuel pin model in parallel two-phase flow. In *Structural mechanics in reactor technology*.

[18] Hara, F. (1979). A theoretical analysis of two-phase flow/fuel pin structural dynamical interactions. In *Structural mechanics in reactor technology. Transactions. Vol. B*.

[19] Li, F., An, C., Duan, M., and Su, J. (2020). Combined damping model for dynamics and stability of a pipe conveying two-phase flow. *Ocean Engineering*, 195:106683.

[20] Liu, G. and Wang, Y. (2018). Natural frequency analysis of a cantilevered piping system conveying gas–liquid two-phase slug flow. *Chemical Engineering Research and Design*, 136:564–580.

[21] LONG, R. (1955). Experimental and theoretical study of transverse vibration of a tube containing flowing fluid. *Journal of Applied Mechanics*, 22:65–68.

[22] Monette, C. and Pettigrew, M. (2004). Fluidelastic instability of flexible tubes subjected to two-phase internal flow. *Journal of fluids and structures*, 19(7):943–956.

[23] Naguleswaran, S. and Williams, C. (1968). Lateral vibration of a pipe conveying a fluid. *Journal of Mechanical Engineering Science*, 10(3):228–238.

[24] Paidoussis, M. (1970). Dynamics of tubular cantilevers conveying fluid. *Journal of Mechanical Engineering Science*, 12(2):85–103.

[25] Paidoussis, M. P. and Issid, N. (1974). Dynamic stability of pipes conveying fluid. *Journal of sound and vibration*, 33(3):267–294.

[26] Païdoussis, M. P. (2014). *Fluid-Structure Interactions: Slender Structures and Axial Flow*, volume 1. Academic press.

[27] Pettigrew, M. and Taylor, C. (2003a). Vibration analysis of shell-and-tube heat exchangers: an overview—part 1: flow, damping, fluidelastic instability. *Journal of Fluids and Structures*, 18(5):469 – 483. Arrays of Cylinders in Cross-Flow.

[28] Pettigrew, M. and Taylor, C. (2003b). Vibration analysis of shell-and-tube heat exchangers: an overview—part 2: vibration response, fretting-wear, guidelines. *Journal of Fluids and Structures*, 18(5):485 – 500. Arrays of Cylinders in Cross-Flow.

[29] Thurman, A. and Mote Jr, C. (1969). Nonlinear oscillation of a cylinder containing a flowing fluid.